Gamow-Teller matrix elements from the ^{12}C$(d,^2$He$)$ and ^{24}Mg$(d,^2$He$)$ reactions at 170 MeV

S. Rakers, C. Bäumer, D. Frekers, and R. Schmidt
Institut für Kernphysik, Westfälische Wilhelms-Universität Münster, D-48149 Münster, Germany

A. M. van den Berg, V. M. Hannen,* M. N. Harakeh, M. A. de Huu, and H. J. Wörtche
Kernfysisch Versneller Instituut, Rijksuniversiteit Groningen, NL 9747 AA Groningen, The Netherlands

D. De Frenne, M. Hagemann, J. Heyse, and E. Jacobs
Vakgroep Subatomaire en Stralingsfysica, Universiteit Gent, B-9000 Gent, Belgium

Y. Fujita
Department of Physics, Osaka University, Toyonaka, Osaka 560-0043, Japan
(Received 8 October 2001; published 2 April 2002)

The ^{24}Mg$(d,^2$He$)^{24}$Na and the ^{12}C$(d,^2$He$)^{12}$B charge-exchange reactions have been studied at an incident energy of 170 MeV. The two protons in the $^1S_0(pp)$ state (indicated as ^{2}He) were both momentum analyzed and detected by the same spectrometer and detector. Background-free ^{2}He spectra with a resolution of about 150 keV (full width at half maximum) have been obtained allowing identification of many levels in the residual nucleus with high precision. It is found that the $(d,^2$He$)$ reaction at 0° is largely governed by the Gamow-Teller (GT) transition operator for the β^+ direction, which makes the reaction selective for isovector 1^+ transitions. In the case of ^{24}Mg, the reaction is compared with (p,n) reaction data in which the same levels in the analog nucleus ^{24}Al are populated. Angular distributions of cross sections for the $(d,^2$He$)$ reaction are presented and compared with distorted-wave Born approximation calculations. GT matrix elements are deduced. A level-by-level comparison with shell-model calculations using the universal *s-d* interaction has been performed. Comparison with (p,p') data yields a level scheme for the $A=24$ isospin triplet.

DOI: 10.1103/PhysRevC.65.044323 PACS number(s): 21.10.Hw, 21.10.Pc, 24.10.Eq, 27.30.+t

I. INTRODUCTION

Spin-isospin-flip excitations in nuclei at vanishing momentum transfer are generally referred to as Gamow-Teller (GT) transitions. They are being studied because the simplicity of the excitation makes them an ideal probe for testing nuclear structure models. But also in astrophysics, GT transitions provide an important input for model calculations of supernovae and element formation, as they are connected to the weak transition strength that drives the explosion dynamics of a massive star at the end of its lifetime [1].

GT transitions in the β^- direction (also referred to as isospin lowering $T_<$ direction) have been studied extensively through (p,n) and $(^3$He$,t)$ charge-exchange reactions [2–6]. The generally good resolution allows easy extraction of the GT distribution and the total $B(GT^-)$ strength in the final nucleus. On the other hand, determination of $B(GT^+)$ strength through a charge-exchange reaction in the $T_>$ direction is considerably more difficult. The neutron beams, which were used in the pioneering experiments at TRIUMF were produced as secondary beams through the ^{7}Li(p,n) reaction [7]. However, the ^{7}Li(p,n) reaction would also leave the ^{7}Be nucleus at high excitation requiring complicated unfolding procedures when generating final (n,p) spectra. Typical values for the resolution obtained were of the order of 1 MeV. More recently, secondary triton beams at sufficiently high energies have become available, which allow the study of GT transitions rather competitively through the $(t,^3$He$)$ reactions [8]. The $(d,^2$He$)$ reaction is another and potentially even more powerful tool to explore the spin-isospin-flip transitions in the $T_>$ direction and has been used in Refs. [9–13].

The interest in studying GT reactions in the $T_>$ direction is twofold. First, the summed strength S_{β^-} for the $T_<$ and S_{β^+} for the $T_>$ direction are connected through the Ikeda sum rule $S_{\beta^-}-S_{\beta^+}=3(N-Z)$ [14,15], and second and more importantly, the $B(GT^+)$ strength distribution is connected to the rate of the electron capture process during the collapse of a massive star, which in turn determines the rate of deleptonization and ultimately the explosive power of a supernova. Whereas, testing the Ikeda sum rule requires extraction of GT strength also in the continuum region where higher multipoles and $2\hbar\omega$ excitations can severely mask the signal [16], the relevance in the latter case is mostly confined to the easy to analyze low excitation region.

In this paper, the $(d,^2$He$)$ reaction with an energy resolution of the order of 150 keV is presented to determine GT matrix elements in the $T_>$ direction for a series of individual states. We denote ^{2}He as two protons coupled to an unbound $^1S_0(pp)$, $T=1$ state. The $^1S_0(pp)$ phase shift exhibits a resonancelike structure near $\varepsilon=0.5$ MeV, where ε denotes the internal energy of the two-proton final-state system. If ε is kept low enough (i.e., below 1 MeV), higher-order partial waves will not significantly contribute to the final-state interaction, thereby leaving "^{2}He" in a well-defined quantum state. Typically, if the two protons are being analyzed in the

*Present address: SRON, Sorbonnelaan 2, 3584 CA Utrecht, The Netherlands.

same magnetic spectrometer, the limited momentum acceptance will guarantee the low ε condition, and as the incident deuteron is a rather pure $^3S_1$ $(T=0)$ state, the $(d,^2\mathrm{He})$ reaction is of isovector spin-flip type with a cross section, which is, apart from the deuteron *D*-wave component, equivalent to that of the corresponding (n,p) reaction multiplied with the spin-flip probability S_{nn} [17]. In the case of vanishing momentum transfer, the $(d,^2\mathrm{He})$ reaction proceeds through the $\boldsymbol{\sigma\tau}$ part of the effective interaction. The measured cross section will then directly be proportional to the $B(GT)$ strength, which in the (n,p) case is [18,19]

$$\frac{d\sigma(q=0)}{d\Omega}=\left(\frac{\mu}{\pi\hbar^2}\right)^2\frac{k_f}{k_i}N_D\ \ J^2_{\sigma\tau}\ \ B(GT^+). \qquad (1.1)$$

$J_{\sigma\tau}$ is the volume integral of the spin-dependent isovector central part of the effective nucleon-nucleon interaction at $q=0$ and can be obtained from Ref. [20]. The distortion factor N_D is usually estimated by calculating the ratio of the distorted-wave (DW) and plane-wave (PW) cross sections,

$$N_D=\frac{\sigma_{DW}(q=0)}{\sigma_{PW}(q=0)}. \qquad (1.2)$$

The cross section $d\sigma(q=0)/d\Omega$ is obtained by extrapolating the measured cross section to $q=0$ using a DWBA (distorted-wave Born approximation) model calculation. This is a reliable procedure if measurements are being performed in a region close to 0°,

$$\frac{d\sigma(q=0)}{d\Omega}=\frac{\sigma_{calc}(q=0)}{\sigma_{calc}(\Theta,q)}\,\frac{d\sigma_{exp}(\Theta,q)}{d\Omega}. \qquad (1.3)$$

For the $(d,^2\mathrm{He})$ reaction a similar approach can be taken, where the only complication arises from the ^{2}He unbound state. The $(d,^2\mathrm{He})$ experimental cross section can be expressed as [11]

$$\left(\frac{d\sigma}{d\Omega}\right)_{(d,^2\mathrm{He})}=\frac{1}{2}\int_{4\pi}\int_{\varepsilon_{min}}^{\varepsilon_{max}}\frac{d^3\sigma}{d\Omega_{^2\mathrm{He}}\,d\Omega_{pp}d\varepsilon}d\Omega_{pp}d\varepsilon, \qquad (1.4)$$

where the integration limits are taken as $\varepsilon_{min}=0$ MeV and $\varepsilon_{max}=1$ MeV, as *P*-wave contributions to the (pp) final state are still negligible in this range [21]. The factor 1/2 accounts for double counting. The evaluation of the integral requires a calculation of the effective solid angle of the spectrometer as a function of the internal energy ε averaged over all possible momenta of the two protons from the ^{2}He decay. This is done by employing a Monte Carlo simulation with the ion-optical parameters of the spectrometer as input for each spectrometer setting and a model for the final-state interaction. The details of such a procedure are given in Ref. [22].

As the $(d,^2\mathrm{He})$ cross section depends on the range of integration over the ^{2}He internal energy ε, and further, because of the likely more complicated nature of the $(d,^2\mathrm{He})$ reaction mechanism, there is an additional calibration factor *C* needed to relate the measured $(d,^2\mathrm{He})$ cross section to the $B(GT^+)$ strength in a similar way as expressed in Eq. (1.1). For a one-step process, one can further assume *C* to be independent of the target mass *A*.

Invoking the appropriate kinematic factors and the $\boldsymbol{\sigma\tau}$ effective interaction at the correct incident energy per nucleon together with the prescription for evaluating the optical-model distortion factor, Eq. (1.1) reads

$$\left(\frac{d\sigma(q=0)}{d\Omega}\right)_{(d,^2\mathrm{He})}=C\times\left[\left(\frac{\mu}{\pi\hbar^2}\right)^2\frac{k_f}{k_i}N_D J^2_{\sigma\tau}B(GT^+)\right]. \qquad (1.5)$$

The factor *C* can be determined by comparing the $(d,^2\mathrm{He})$ cross sections with known GT strength from β decay, where available, or by using the $(d,^2\mathrm{He})$ reaction on self-conjugate nuclei like, e.g., ^{24}Mg, where the GT strength is expected to be the same in both isospin directions

$$B(GT^-)=B(GT^+), \qquad (1.6)$$

so that in this case, $B(GT^-)$ data from (p,n) experiments can be taken as a reference.

In the case of the $^{12}\mathrm{C}(d,^2\mathrm{He})$ reaction, the $B(GT)$ value for the ^{12}B ground-state transition can be evaluated from (p,n) [5] and (n,p) [23,24] experiments as well as from the β decay log *ft* value [25]. However, it is known that the *ft* values for the transition to the ^{12}C ground-state for both β decay directions differ by about 10% [26]. Therefore, a comparison with the $B(GT)$ value from the $^{12}\mathrm{B}(\beta^-)^{12}\mathrm{C}$ decay may be more appropriate for the present situation than taking the (p,n) or (n,p) data. In the case of the $^{24}\mathrm{Mg}(d,^2\mathrm{He})^{24}\mathrm{Na}$ reaction, there is no similar ground state β transition. High resolution data for transitions to the mirror nucleus ^{24}Al are only available from (p,n) reactions [6], and the symmetry relation of Eq. (1.6) is then used for comparison.

All $B(GT)$ values mentioned in the present paper are in units where $B(GT)=3.0$ for the β decay of the free neutron.

II. EXPERIMENT

The present experiments were carried out using the ESN detector [27–29], which consists of a focal-plane detection system comprising two vertical drift chambers, and a tracking detector which is a set of four multiwire proportional chambers. The detector is located near the focal plane of the Big-Bite spectrometer (BBS) [30]. The instrument was primarily built as a proton polarimeter, but has also been shown to be an excellent ^{2}He detection facility. A full account of how the $(d,^2\mathrm{He})$ experiments are being performed and analyzed can be found in Ref. [22].

170 MeV deuterons were delivered by the AGOR cyclotron. The spectrometer and the beam line were set up in dispersion-matched mode to ensure good momentum resolution. Self-supporting targets with high enrichment were used. The thicknesses were 9.4 mg/cm^2 for ^{12}C (98.9%), and 7.0 mg/cm^2 for ^{24}Mg (99.9%). Beam currents were measured by a Faraday cup. They ranged from about 0.2 nA to 5.0 nA, depending on the spectrometer angle. The detector efficiency for two-particle events including the tracking effi-

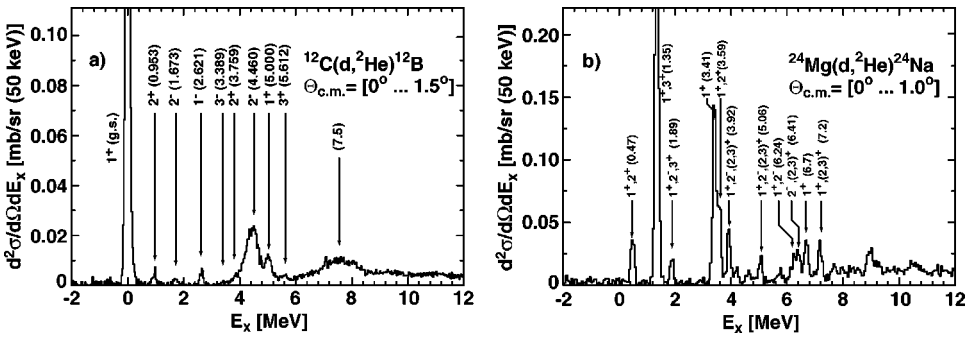

FIG. 1. Excitation energy spectra near 0° of ^{12}B (a) and ^{24}Na (b). The energy levels of known J^π states in ^{12}B are taken from Ref. [32], while the displayed ^{24}Na levels are from the present experiment. The spectra have been obtained at a spectrometer angle setting $\Theta_{BBS}=0°$, which corresponds to a center-of-mass angle range indicated in the square brackets.

ciency of the analysis software has been evaluated to be 90%. Measurements were made at three different spectrometer angle settings covering an angular range in the laboratory system from 0° to 5°. The ^{12}C measurement included five further settings between 15° and 27°. For the three forward angle settings, each data set was divided into two angular bins of equal size.

For the extraction of cross sections we made use of a peak-fitting program [31]. Spectra were fitted by using Gaussian peak shapes. The quoted errors in cross sections are due to counting statistics and due to a statistical component in the Monte Carlo calculation for the acceptance correction, which is about 5%. An additional systematic error due to target thickness, current integration, etc., is estimated to be 10% at most.

The dispersion of the spectrometer was calibrated using the ^{12}C(p,p') reaction [27]. The accuracy of ^{2}He excitation energy was verified by comparing the obtained ^{12}C$(d,^2$He$)^{12}$B spectrum (Fig. 1) to literature values [32]. The ^{24}Na spectrum was calibrated by matching the energy of the strongest peak to the known state at 1.35 MeV [33]. We estimate the error of the excitation energy of identified peaks to be about 20 keV.

Fig. 1 shows excitation energy spectra of the examined nuclei at $\Theta_{BBS}=0°$. The measured data have been treated as described in Ref. [22]. We note that the spectra are free of any instrumental background or background due to random correlations. The resolution is 165 keV full width at half maximum (FWHM) for the ^{12}C, and 145 keV (FWHM) for the ^{24}Mg target. Both nuclei have recently been subject to $(d,^2$He) experiments by other groups [12,34,35], too, yet resolution was usually not better than 650 keV, so that peak-by-peak comparisons are difficult.

The good resolution allows identification of a series of excited states in both daughter nuclei. Spectra have been analyzed up to excitation energies of 7.2 MeV, where the density of states is still low enough to analyze single peaks.

In the ^{12}B nucleus, 1^+ peaks are located at 0 MeV (ground state) and at 5.00 MeV. Pure 1^+ strength in ^{24}Na is located at 3.41 MeV and 6.70 MeV. The peaks at 0.47 MeV, 1.35 MeV, 3.59 MeV, and 6.24 MeV are mainly 1^+, but contain small contributions from overlapping different states. Their $\Delta L=0$ fractions at 0° are more than 80% of the total cross section. Several other peaks (1.89 MeV, 3.92 MeV, 5.06 MeV, and 7.2 MeV) still carry some $\Delta L=0$ strength. The J^π assignments have been verified by comparing angular distributions to DWBA calculations, as is described below.

III. DWBA ANALYSIS

For the analysis of the measured data, DWBA and PWBA calculations have been performed to evaluate the distortion factor that relates the $B(GT)$ strength value to the zero momentum transfer cross section [Eqs. (1.1) and (1.2)]. For overlapping peaks, it has been used to extract the $\Delta L=0$ contribution by applying a multipole decomposition using the distinct shape of each part.

For the calculations we utilized the ACCBA code of Okamura [36], which is specialized for the $(d,^2$He) reaction. It applies an ordinary DW formalism in the incident channel and treats the three-body problem in the exit channel in the adiabatic approximation. This approach is relatively simple and a parameter-free method. The spin-orbit potential is not included. However, it is not likely to play an important role near $q=0$ anyway. The code handles the D-wave contributions of the incident deuteron and the outgoing ^{2}He by solving coupled-channel equations, however, the impact is small and hardly noticeable [36].

For the calculation, deuteron and proton optical model parameters by Bäumer *et al.* [37] ($d+^{12}$C, $d+^{24}$Mg at 170 MeV), Comfort and Karp [38] ($p+^{12}$C interpolated to 80 MeV), and Olmer *et al.* [39] (taken from $p+^{28}$Si at 80 MeV), were used. One may point out that the reaction calculations are quite insensitive to variations of the optical model parameters within reasonable bounds. For the effective interaction, we performed a smooth interpolation of the free *NN* *t*-matrix parametrizations by Franey and Love [40] between 50 and 175 MeV (i.e., four points) to a projectile energy of 85 MeV per nucleon. At bombarding energies below 100 MeV per nucleon, a *g*-matrix approach may be an appropriate alternative, however, *t*-matrix parametrizations are readily available, and the impact of the choice of the interaction on the GT strength extraction from near 0° cross section data is not expected to be significant.

Nuclear wave functions and one-body transition densities (OBTDs) were generated by the shell-model code OXBASH [41] using the *p* model space and the residual interaction by Cohen and Kurath [42] for the ^{12}C case. For the ^{24}Mg case, the *s-d* model space and the ''universal *s-d*'' residual interaction of Brown and Wildenthal [43,44] were employed to

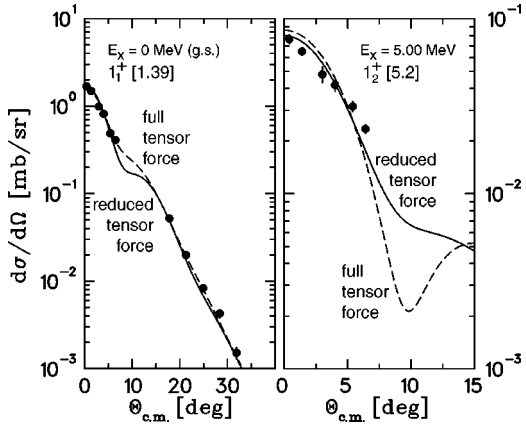

FIG. 2. Experimental ^{12}C(d,^{2}He)^{12}B differential cross sections for the two 1^+ states at 0 and 5.00 MeV (dots) and theoretical calculations. The solid line depicts the DWBA calculation with the reduced tensor force; the dashed line represents a calculation with the full tensor interaction. The state at 5.00 MeV is masked by a strong spin-dipole resonance at 4.5 MeV at higher angles, so that only the data points of low angular settings are shown. The used shell-model wave functions are shown as subscripts of J^π labels, the scaling factors of DWBA curves are in square brackets.

generate the positive-parity wave functions. Negative-parity states can be assumed to originate from transitions between the p shell and s or d subshells, which necessitates calculations in an enlarged model space. With the untruncated p-s-d model space, one needs to include 20 valence particles, which makes the calculations impossible with the present code. We truncated the model space by assuming completely filled $1p_{3/2}$ subshells for both neutrons and protons. This reduces the number of valence particles to 12, which makes the calculation feasible. For the residual interaction, the ''PSDMWK'' interaction was used [43–46]. The calculated se-

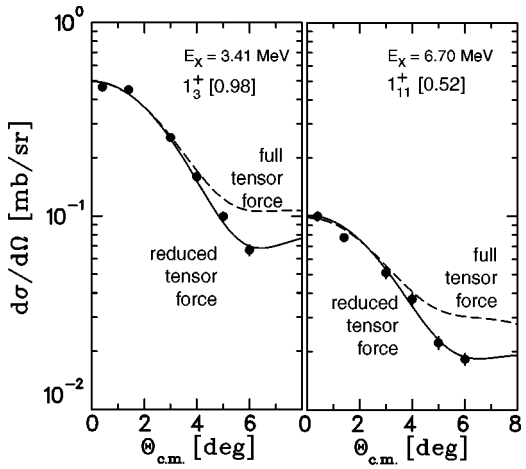

FIG. 3. Experimental ^{24}Mg(d,^{2}He)^{24}Na differential cross sections for the pure 1^+ states at 3.41 MeV and 6.70 MeV (dots) and theoretical calculations. The solid line represents the calculation with the reduced tensor force, the dashed line a calculation with the full tensor interaction. DWBA calculations are scaled by the factors indicated in square brackets. The J^π subscripts indicate the shell-model wave functions used.

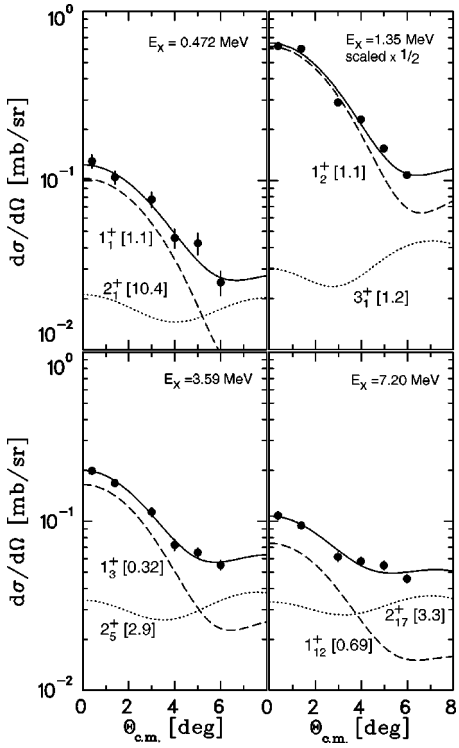

FIG. 4. Experimental ^{24}Mg(d,^{2}He)^{24}Na differential cross sections for four strong peaks at 0.47 MeV, 1.35 MeV, 3.59 MeV, and 7.20 MeV, which have dominant 1^+ contributions but are contaminated by higher multipole transitions. The 1^+ calculation is illustrated by the dashed line, the 2^+ or 3^+ calculations by the dotted line. The solid line is the sum. DWBA scaling factors are in square brackets. The J^π subscripts indicate the shell-model wave functions used.

ries of 2^- levels reproduces known levels in ^{24}Na satisfactorily, however, transitions are described rather simply by only two OBTDs.

For the DWBA calculations of individual transitions, we chose the shell-model wave functions of those states whose excitation energies and strength values are closest to experiment.

1^+ states can be excited via the central $\boldsymbol{\sigma\tau}$ interaction ($\Delta L=0$ component) but also by the isovector tensor interaction ($\Delta L=2$ component). The latter defines the slope of the calculated curve at the diffraction minima. We mention here that for the ^{24}Mg case the tensor force needed to be lowered by a factor of two in order to get a good fit at the first diffraction minimum. For the illustration of this feature, calculations with both full and reduced tensor force are shown for all pure 1^+ states, regardless if in ^{12}B or ^{24}Na (Figs. 2 and 3). Calculations intended for mixed state decomposition were consistently performed with the reduced tensor force (Fig. 4).

In Fig. 2 we show the experimental angular distributions for the two 1^+ peaks in ^{12}B compared to the respective DWBA calculations. The strong ground state transition has been measured up to 32°, but the state at 5.00 MeV is comparatively weak and, therefore, masked by the adjacent spin-dipole resonance at 4.5 MeV at angles greater than 6°.

The experimental differential cross sections of both transitions to ^{12}B can be reasonably well fitted by both calculations, either with reduced or full tensor force. The calculations of the 1^+ state at 5.00 MeV show the special feature that the tensor force acts destructively upon the cross section and sharpens the first diffraction minimum, while in all other observed cases it contributes constructively, thereby smearing out the diffraction pattern.

Figure 3 depicts the experimental angular distributions as well as the respective calculations for the two states in ^{24}Na at 3.41 MeV and 6.70 MeV, which we assume to be pure 1^+ states. The assumption is based on the characteristic steep fall off of the angular distributions. The calculations with the full tensor force for these states exhibit curves (dashed line) which are even not steep enough to fit the experimental distribution. With the tensor part of the effective interaction reduced by a factor of two, the calculations reproduce the experimental data of these states well.

In Fig. 4, the differential cross sections for four strong 1^+ peaks are shown. These peaks are found to be combinations of 1^+ and $2^+/3^+$ states.

The lowest energy peak is composed of a 1^+ state known to be at 472 keV and a 2^+ state at 563 keV [33]. These states cannot be resolved in our experiment, but the centroid of the peak is observed to shift to higher excitation energies with increased scattering angle. The differential cross sections are fitted well by a superposition of the 1^+_1 and a weaker 2^+_1 calculation.

The next peak at 1.35 MeV is the strongest peak in the spectrum and consists of a strong 1^+ state, which is also known from the ^{24}Ne β^- decay, with some higher multipole admixture. A 2^+ and a 3^+ state are known to exist close by, however in the shell model, which also predicts both states, only the 3^+_1 state gives sufficient transition strength. A $1^+_2/3^+_1$ combination is used to fit the differential cross sections.

The peak at 3.59 MeV is interpreted as a superposition of the 1^+_3 and the 2^+_5 states. Here the transition strength of the 2^+_5 state is larger than a similarly close-by lying 3^+ state. We note that within our range of measured angles, contributions of 2^+ and 3^+ states can, of course, not safely be distinguished. However, from the graphs one can see that the $0°$ cross sections, and, thereby, the GT transition strengths, are only slightly affected by the higher multipole contributions.

Finally, the states at 6.24 MeV and 7.20 MeV [cf. Fig. 1(b)] exhibit a rather flat dependence of the cross section with increasing angle (displayed in Fig. 4 only for the peak at 7.20 MeV). They can be fitted by superpositions of $1^+/2^-$ and $1^+/2^+$ calculations, respectively. For the peak at 7.20 MeV, the 2^+ contribution at $0°$ is large compared to the 1^+ fraction.

Full multipole decompositions have been carried out for the peaks that show no prominent $\Delta L=0$ angular distribution. These include the peaks at 1.89 MeV, 3.92 MeV, 5.06 MeV, and 6.41 MeV [see Fig. 1(b)]. Form factors for $\Delta L=0$, $\Delta L=1$ and $\Delta L=2$ have been generated by taking shell-model matrix elements of states in this excitation region as mentioned above. Here, the interpretation of the results may have to be taken with some reservation also because of uncertainties due to model space truncation. The $\Delta L=0$ contributions to the $0°$ cross sections are listed in Table I. All the states in this category are indicated by a superscript "b" in Table I. For the $\Delta L=0$ cross sections extracted in this way, overall errors of 30% have been assumed. The state at 6.41 MeV does not exhibit any $\Delta L=0$ component.

IV. DISCUSSION

In Fig. 5 [upper part (a) and (b)] we first compare the raw ^{24}Mg$(d,^2$He$)^{24}$Na spectrum with that of the analog ^{24}Mg$(p,n)^{24}$Al reaction measured by Anderson *et al.* [6]. One observes a one-to-one correspondence up to a rather detailed level, except for the doublet structure at 3.41 and 3.59 MeV in ^{24}Na, which is not resolved in ^{24}Al, and which one may treat as a single peak. For further illustration purposes, we have plotted the measured ^{24}Mg$(d,^2$He) cross section versus the extracted GT^- strength from the ^{24}Mg(p,n) reaction in the lower part of the figure [Fig. 5(c)]. Although a near perfect linear relationship over a wide range of energies is truely remarkable, such a plot may indeed be deceiving. This is especially true, if different target nuclei are being combined in such a way (as, e.g., shown in Refs. [12,35]), because the different kinematic and distortion factors involved are then being ignored. There may, however, be fortuitous situations where these factors cancel, as it also happens in our case, e.g., for the 5.00 MeV level in ^{12}C and the 0.47 MeV level in ^{24}Mg when referring to Table I, where cross sections and $B(GT)$ values happen to be identical.

For a consistent analysis, distortion factors N_D were computed using again the ACCBA code. PWBA cross sections have been obtained by setting the optical model potential strengths to zero. The results for the present $(d,^2$He) reaction averaged over the excitation region under consideration are $N_D=0.229\pm0.005$ for ^{12}C and $N_D=0.160\pm0.003$ for ^{24}Mg, where the uncertainties indicate the largest variations over the energy. The volume integral of the effective central $\boldsymbol{\sigma\tau}$ interaction at $E/A=85$ MeV has been taken to be $|J_{\boldsymbol{\sigma\tau}}|=165$ MeV fm^3 [20]. The fractions $\sigma_{l=0}/\sigma_{tot}$ defining the pure $\Delta L=0$ contributions in the various peaks have been evaluated for $q=0$ in DWBA. We note that even for pure 1^+ states, these are not unity owing to the small $^3D_1$ admixture of the wave function of the incident deuteron .

Individual calibration factors C_i have then been determined from the experimental cross sections (here the fraction for $\Delta L=0$) by using Eq. (1.5) and the $B(GT^-)$ values from the ^{12}B β^- decay [25] and the ^{24}Mg(p,n) reaction [6]. These are listed in Table I. For the strongest peaks, the individual factors are close to each other, while for some weak or mixed transitions (especially the 5.06 and 7.20 MeV states in ^{24}Na) deviations are comparatively large.

The "universal" A-independent calibration factor C has been extracted by using the ground state transition in ^{12}B and the five strongest and purest 1^+ transitions in ^{24}Na. The cross section weighted average value is

$$C=0.267\pm0.017.$$

TABLE I. GT strength known from $^{12}B(\beta^-)^{12}C$ and $^{24}Mg(p,n)$ reactions [6,25], and experimental cross sections, distortion factors N_D, proportionality factors C_i, and extracted $B(GT^+)$ values from the present $^{12}C(d,^2He)$ and $^{24}Mg(d,^2He)$ experiments. For the ratios $\sigma_{l=0}/\sigma_{tot}$ refer to the text. The errors are statistical errors only, except, the numbers in the second error column of the extracted $B(GT^+)$ values reflect the errors from the calibration factor, which are of systematic nature. The overall systematic error due to target thickness, beam current integration, etc. (see text) is not included.

Target	Reference data [6,25]		Present data					
	E_x [MeV]	$B(GT^-)$	E_x [MeV]	$d\sigma/d\Omega$(q=0) [mb/sr]	$\sigma_{l=0}/\sigma_{tot}$ (q=0)	N_D	C_i	$B(GT^+)$ using $C=0.267$
^{12}C	0.00	0.998	0.00	2.580 ± 0.138	0.988	0.229	0.249[a]	$0.930\pm0.050\pm0.059$
^{12}C			5.00	0.138 ± 0.010	0.976	0.229		$0.050\pm0.004\pm0.003$
^{24}Mg	0.44	0.050	0.47	0.138 ± 0.012	0.821	0.160	0.263[a]	$0.049\pm0.004\pm0.003$
^{24}Mg	1.07	0.613	1.35	1.563 ± 0.085	0.948	0.160	0.284[a]	$0.654\pm0.035\pm0.042$
^{24}Mg	1.58[b]	0.020	1.89[b]	0.087 ± 0.026	0.649	0.160	0.334	$0.025\pm0.008\pm0.002$
^{24}Mg	2.98	0.362	3.41	0.667 ± 0.039	0.980	0.160	0.284[a]	$0.290\pm0.016\pm0.018$
			3.59	0.266 ± 0.018	0.806	0.160		$0.095\pm0.006\pm0.006$
^{24}Mg	3.33	0.059	3.92[b]	0.193 ± 0.058	0.809	0.160	0.396	$0.070\pm0.022\pm0.004$
^{24}Mg	4.69[b]	0.015	5.06[b]	0.093 ± 0.027	0.561	0.160	0.427	$0.024\pm0.007\pm0.002$
^{24}Mg			6.24[b]	0.086 ± 0.026	0.818	0.160		$0.031\pm0.010\pm0.002$
^{24}Mg	6.46	0.068	6.70	0.161 ± 0.012	0.972	0.160	0.277[a]	$0.071\pm0.005\pm0.004$
^{24}Mg	6.87	0.029	7.20	0.173 ± 0.013	0.642	0.160	0.460	$0.050\pm0.004\pm0.003$
^{24}Mg	Sum	1.216					Sum	$1.359\pm0.048\pm0.087$

[a]Value taken for determination of universal calibration factor C.

[b]Indicates value obtained from multipole decomposition.

This factor was subsequently applied to all transitions, including the weaker and strongly mixed ones, to determine their individual GT^+ strength and, consequently, the total summed strength.

Table I shows the extracted individual GT^+ strength of the various states in ^{12}B and ^{24}Na and a comparison of the summed $B(GT)$ strength for transitions from ^{24}Mg. Of course, the summed GT strength for the transitions to ^{24}Na is the same as the one observed for ^{24}Al within a standard deviation when considering the same levels. The summed strength is also consistent with the value determined from the $^{24}Mg(n,p)$ reaction by Richter *et al.* [47]. The total $B(GT)$ strength predicted by the shell model for the considered excitation energy region is 2.1. Compared to the experimental value of 1.359, this corresponds to a quenching factor of 0.65.

The experimentally extracted $B(GT)$ values for $A=24$ are compared with the results from the shell-model calculation for individual levels in Fig. 6. Using the USD residual interaction [43,44], the calculation describes the GT strength distribution for excitations up to about 7 MeV well. The notable exception is the doublet structure at 3.41/3.59 MeV in ^{24}Na seen in the experiment, for which the USD interaction predicts only one state. However, the predicted state is strong enough to account for the strength of the doublet even when the quenching factor is taken into account. At higher excitation energies, the shell-model calculation yields two states that correspond to the two measured states at 6.7 and 7.2 MeV, however, their calculated $B(GT)$ strength is considerably overestimated.

As mentioned earlier, we had to adjust the tensor interaction strength to fit our differential cross sections. The adjustment was the same for both examined nuclei and was independent of the momentum transfer. The tensor force is the least well known component of the effective interaction, and it is conceivable that the employed parameterization by Franey and Love [40] overestimates the strength. It is also possible that the tensor force is suppressed in the $(d,^2He)$ reaction at the bombarding energy used in our experiments. It would be desirable that further effort be put into the explanation of this effect, e.g., by the study of stretched-state excitations, which are mediated predominantly by the tensor force [48]. On the other hand, Okamura *et al.* used for their $^{12}C(d,^2He)$ analysis a nonmodified *t* matrix at 140 MeV and achieved a good description of the experimental angular distributions [36]. However, the effect of the tensor force for $A=12$ nuclei may be too small (cf. Fig. 2) to draw any conclusions. Of course, calculations using a *g*-matrix approach remain a viable future option. At present, however, such a calculation lies outside the scope of this paper.

Finally, a comparison of $(d,^2He)$, (p,n), and (p,p') data [6,49,50] for the $A=24$ triad has been carried out for the states populated by $(\Delta L=0,\ \Delta S=1,\ \Delta T=1)$ transitions. The relative strength of the cross sections have been taken as a reference for relating the analog states in the isospin triplet, and only the strongest states have been considered. Figure 7 shows the level schemes of the three nuclei ^{24}Na, ^{24}Mg, and ^{24}Al. The excitation energies in the ^{24}Mg are offset by 9.52 MeV. Due to isospin symmetry, almost all strong 1^+ states can be related among the three $A=24$ nuclei.

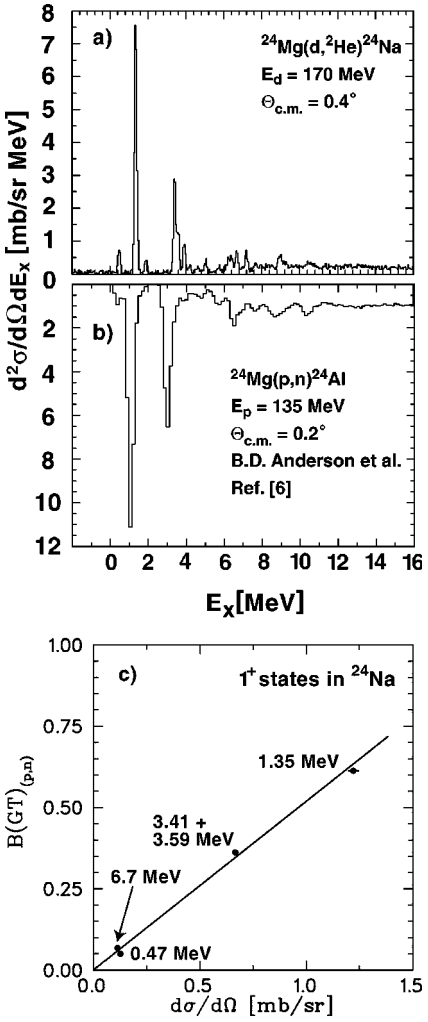

FIG. 5. (a), (b) Direct comparison of $(d,^2\mathrm{He})$ and (p,n) spectra. (c) $(d,^2\mathrm{He})$ cross sections at $\Theta_{\mathrm{c.m.}}=0.4°$ of states in ^{24}Na plotted versus GT^- strength in ^{24}Al. The respective states are marked by their excitation energy in ^{24}Na.

Analog states are connected by the dashed lines. We note that the doublet at 3.41/3.59 MeV seen by us is also present in the (p,p') case, but the peaks seem to merge to a single state in ^{24}Al, or at least come too close to be resolved in the (p,n) experiment. This interpretation is also corroborated by considering the total strength.

A strong 1^+ state in ^{24}Mg at 3.01 MeV (reduced by the offset of 9.52 MeV), which had been given a $T=1$ assignment through (p,p'), has no analog at all, indicating that the $T=1$ assignment may be incorrect.

Further, to connect the 5.06/4.69 MeV states in ^{24}Na/^{24}Al, a possible candidate state at 4.38 MeV in ^{24}Mg (i.e., 13.90 MeV total excitation) is observed in the ^{24}Mg(p,p') experiment by Crawley *et al.* [49] and also in the spectrum of the polarized ^{24}Mg$(\vec{p},\vec{p}\,')$ measurements of Sawafta *et al.* [50]. When multiplied with the spin-flip probability in the latter analysis, only little spin strength remains, and the value may be consistent with the strength observed in the present $(d,^2\mathrm{He})$ and the (p,n) experiments. However, the excitation energy would amount to a Coulomb shift of $+680$ keV in one case and -310 keV in the other. We, therefore, prefer to leave the state unassigned.

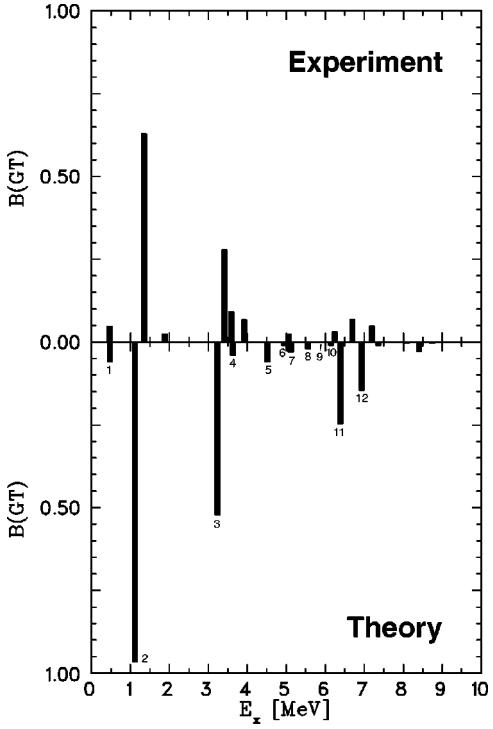

FIG. 6. $B(GT)$ values obtained from USD shell-model calculation (lower part, the small numbers are labels to denote the level number of the calculation), compared with $B(GT)$ values obtained by the present $(d,^2\mathrm{He})$ measurement (upper part).

The weaker states at 1.89/1.58 MeV (^{24}Na/^{24}Al) and 3.92/3.33 MeV also seem to have no partner in ^{24}Mg, which

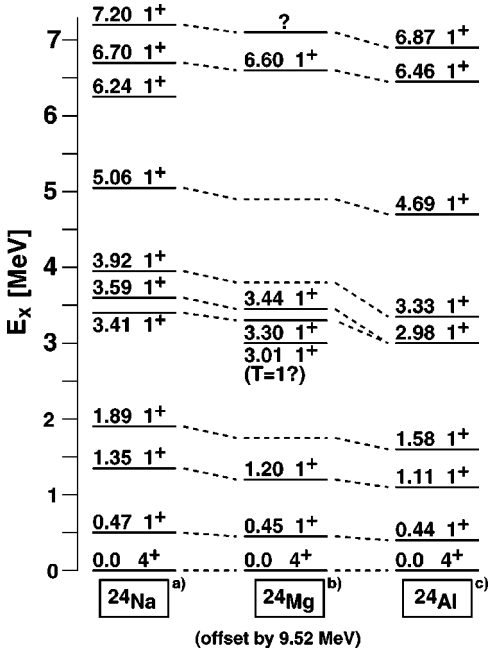

FIG. 7. Corresponding analog states in the $A=24$ triad where (a) shows present data, (b) is data taken from Ref. [49], and (c) is data taken from Ref. [6].

may be due to the fact that the respective excitation energies in ^{24}Mg are around 12 to 13 MeV, and the extraction of angular distributions from weak peaks suffers from the underlying background. Looking at the (p,p') spectrum alone, the states at 7.20/6.87 MeV do seem to have a counterpart in ^{24}Mg, however, no angular distribution and no explicit analysis are published in Refs. [49,50].

V. CONCLUSIONS

Differential cross sections for transitions from ^{12}C and ^{24}Mg in the β^+ direction have been measured by the $(d,^2\mathrm{He})$ reaction. The energy resolution of 160 and 145 keV, respectively, and the angular distributions allow to identify various 1^+ states in the daughter nuclei. Due to the nature of the reaction, these transitions can be identified as GT transitions. Angular distributions of cross section have been analyzed using DWBA semimicroscopic model calculations. Details like higher multipole admixtures or possible overestimation of tensor-interaction strength of the used effective interaction parametrization have been discussed.

The 0° cross sections have been compared to known Gamow-Teller transition strengths, and an A-independent factor relating 0° cross sections to GT^+ strength has been extracted. $B(GT^+)$ values have been determined for states with previously unknown strength.

A further comparison with (p,p') data leads to a level scheme containing the $1^+(T=1)$ levels of the $A=24$ triad, where several analog states could now be related to each other.

ACKNOWLEDGMENTS

We wish to thank S. Brandenburg and the KVI accelerator staff. We thank H. Okamura for providing the ACCBA code. We are particularly grateful to B. D. Anderson who provided us with the ^{24}Mg(p,n) data. This work was performed with support from the Land Nordrhein-Westfalen and the EU under Contract No. TMR-LSF ERBIMGECT980125. It was further performed as part of the research program of the Stichting FOM with financial support from the Nederlandse Organisatie voor Wetenschappelijk Onderzoek and as part of the research program of the Fund for Scientific Research-Flandres.

[1] G.M. Fuller, W.A. Fowler, and J. Newman, Astrophys. J. **293**, 1 (1985); Astrophys. J., Suppl. **48**, 279 (1982); Astrophys. J. **252**, 715 (1982); Astrophys. J., Suppl. **42**, 447 (1980).
[2] H. Akimune *et al.*, Nucl. Phys. **A569**, 245c (1994).
[3] Y. Fujita *et al.*, Phys. Lett. B **365**, 29 (1996).
[4] J. Rapaport *et al.*, Phys. Rev. C **24**, 335 (1981).
[5] B.D. Anderson *et al.*, Phys. Rev. C **36**, 2195 (1987).
[6] B.D. Anderson *et al.*, Phys. Rev. C **43**, 50 (1991); (private communication).
[7] R. Helmer, Can. J. Phys. **65**, 588 (1987).
[8] B.M. Sherrill *et al.*, Nucl. Instrum. Methods Phys. Res. A **432**, 299 (1999).
[9] T. Motobayashi *et al.*, Phys. Rev. C **34**, 2365 (1986).
[10] T. Motobayashi *et al.*, Nucl. Instrum. Methods Phys. Res. A **271**, 491 (1988).
[11] H. Okamura *et al.*, Phys. Lett. B **345**, 1 (1995).
[12] H.M. Xu *et al.*, Phys. Rev. C **52**, R1161 (1995).
[13] C. Ellegaard *et al.*, Phys. Rev. Lett. **59**, 974 (1987).
[14] C. Gaarde *et al.*, Nucl. Phys. **A334**, 248 (1980).
[15] K. Ikeda *et al.*, Phys. Lett. **3**, 271 (1963).
[16] F. Osterfeld, Rev. Mod. Phys. **64**, 491 (1992).
[17] D.P. Stahel *et al.*, Phys. Rev. C **20**, 1680 (1979).
[18] C.D. Goodman *et al.*, Phys. Rev. Lett. **44**, 1755 (1980).
[19] T.N. Taddeucci *et al.*, Nucl. Phys. **A469**, 125 (1987).
[20] W.G. Love and M.A. Franey, Phys. Rev. C **24**, 1073 (1981).
[21] S. Kox *et al.*, Nucl. Phys. **A556**, 621 (1993).
[22] S. Rakers *et al.*, Nucl. Instrum. Methods Phys. Res. A **481**, 253 (2001).
[23] K.P. Jackson *et al.*, Phys. Lett. B **201**, 25 (1988).
[24] N. Olsson *et al.*, Nucl. Phys. **A559**, 368 (1993).
[25] F. Ajzenberg-Selove, Nucl. Phys. **A490**, 1 (1988); **A506**, 1 (1990); **A523**, 1 (1991).
[26] R.E. McDonald *et al.*, Phys. Rev. C **10**, 333 (1974).
[27] H.J. Wörtche, Nucl. Phys. **A687**, 321c (2001).
[28] M. Hagemann *et al.*, Nucl. Instrum. Methods Phys. Res. A **437**, 459 (1999).
[29] B.A.M. Krüsemann *et al.*, IEEE Trans. Nucl. Sci. **47**, 2741 (2001).
[30] A.M. van den Berg, Nucl. Instrum. Methods Phys. Res. B **99**, 637 (1995).
[31] S. Strauch and F. Neumeyer, computer program FIT (TU Darmstadt, Germany, 1995).
[32] F. Ajzenberg-Selove, Nucl. Phys. **A506**, 1 (1990).
[33] P.M. Endt, Nucl. Phys. **A521**, 1 (1990).
[34] T. Niizeki *et al.*, Nucl. Phys. **A577**, 37c (1994).
[35] H. Ohnuma *et al.*, Phys. Rev. C **47**, 648 (1993).
[36] H. Okamura, Phys. Rev. C **60**, 064602 (1999).
[37] C. Bäumer *et al.*, Phys. Rev. C **63**, 037601 (2001).
[38] J.R. Comfort and B.C. Karp, Phys. Rev. C **21**, 2162 (1980).
[39] C. Olmer *et al.*, Phys. Rev. C **29**, 361 (1984).
[40] M.A. Franey and W.G. Love, Phys. Rev. C **31**, 488 (1985).
[41] B. A. Brown *et al.*, computer program OXBASH (unpublished).
[42] S. Cohen and C. Kurath, Nucl. Phys. **A73**, 1 (1965).
[43] B.H. Wildenthal, Prog. Nucl. Phys. **11**, 5 (1984).
[44] B.A. Brown and B.H. Wildenthal, Phys. Rev. C **27**, 1296 (1983).
[45] D.J. Millener and D. Kurath, Nucl. Phys. **A255**, 315 (1975).
[46] D. J. Millener (private communication), as cited in OXBASH interaction files, 1984.
[47] A. Richter *et al.*, Phys. Rev. Lett. **65**, 2149 (1990).
[48] R. Pourang *et al.*, Phys. Rev. C **47**, 2751 (1993).
[49] G.M. Crawley *et al.*, Phys. Rev. C **39**, 311 (1989).
[50] R. Sawafta *et al.*, Phys. Lett. B **201**, 219 (1988).